Ocean Sci. Discuss., doi:10.5194/os-2017-30, 2017
Manuscript under review for journal Ocean Sci.
Discussion started: 15 May 2017

Ocean Science Discussions
Open Access
EGU

Turbulent Length Scales in a Fast-flowing, Weakly Stratified, Strait: Cook Strait, New Zealand

Craig L. Stevens[1,2]

[1] National Institute of Water and Atmospheric Research, Greta Point, Wellington, 6021, New Zealand.
[2] Department of Physics, University of Auckland, New Zealand

Correspondence to: Craig Stevens (craig.stevens@niwa.co.nz)

Abstract. There remains much to be learned about the full range of turbulent motions in the ocean. Here we consider turbulence and overturn scales in the relatively shallow, weakly stratified, fast-flowing tidal flows of Cook Strait, New Zealand. With flow speeds reaching 3 m s^{-1} in a water column of ~300 m depth the location is heuristically known to be highly turbulent. Dissipation rates of turbulent kinetic energy ε, along with the Thorpe scale, L_T, are described. Thorpe scales, often as much as one quarter of the water depth, are compared with dissipation rates and background flow speed. Turbulent energy dissipation rates ε are modest but high for oceans, around 5×10^{-5} W kg^{-1}. Comparison of the buoyancy-limit Ozmidov scale L_{Oz} suggest the Cook Strait data lie for the majority of the time in the $L_{Oz}>L_T$ regime, but not universally. Also, comparison of direct and L_T -based estimates of ε exhibit reasonable similarity.

1 Introduction

It is well-established that turbulent mixing in the ocean is patchy (see Waterhouse et al. 2012 for a synthesis). Thus, there is substantial benefit in seeking out extreme conditions to fully capture the global energy budget. Tidal motion, through one pathway or another, drives significant mixing in the ocean. While is it understood that this can influence coastal environments (e.g. Wesson and Gregg 1994), knowledge gained in

Ocean Sci. Discuss., doi:10.5194/os-2017-30, 2017
Manuscript under review for journal Ocean Sci.
Discussion started: 15 May 2017

shallow coastal situations is also applicable in deeper ocean conditions (e.g. Dale and Inall 2015). Here we consider these issues in the fast flows of a large tidally-driven passage, Cook Strait, a situation that couples a relatively large vertical extent with large inertial forcing.

In a 1999 paper reviewing the first shear probe measurements of oceanic turbulence Stewart and Grant (1999) described the flows in Discovery Passage as sustaining Reynolds Numbers (Re) amongst the largest in the universe. True or not, it is a useful benchmark and discussion point. There is a tendency to ignore Reynolds number in geophysical flows as they are typically so very large, primarily because of the length scales involved. Cook Strait has comparable flow speeds to Discovery Passage but is around four times the depth, and so suggests a larger bulk Re. From the diapycnal diffusion perspective, despite this highly turbulent large scale flow, stratification clearly persists through the strait (Stevens 2014).

Of practical concern here is the amount of kinetic energy lost from the system via dissipation (i.e. the rate of dissipation of turbulent kinetic energy, ε) as this plays an important role in adequately simulating ocean systems where there is a high dynamic range of variability. This then informs quantification of turbulent diapycnal diffusion which is a balance of turbulent overturning against a stably-stratified background as characterised by the buoyancy frequency squared $N2=(g/\rho)(d\rho/dz)$. Wesson and Gregg (1994) set the scene for the research theme surveying turbulence quantities in the exchange-dominated Straits of Gibraltar where they were able to quantify key turbulence parameters as driven both by internal shear and boundary mixing.

Mater and Venayagamoorthy (2014) lay out a pictorial representation of length scales in stratified turbulence. The observed Thorpe overturning scale, L_T, is a relatively measurable quantity associated with ocean structure and can be considered the energy baring scale. This is contained by the Ozmidov scale ($L_{Oz}=[\varepsilon/N^3]^{1/2}$) that identifies the limits to growth of eddies and also the Kolmogorov length scale ($L_K=[\nu^3/\varepsilon]^{1/4}$, ν is kinematic molecular viscosity) where turbulent fluctuations are absorbed by viscous damping forces.

Ocean Sci. Discuss., doi:10.5194/os-2017-30, 2017
Manuscript under review for journal Ocean Sci.
Discussion started: 15 May 2017

It is common to seek to relate the observable L_T to mechanistically relevant quantities like turbulent kinetic energy, and its dissipation rate ε (e.g. Dillon 1982; Mater et al. 2015). This enables properties estimated from ε, *N* and velocity *Sh* to be inferred from relatively achievable measurements. Recently Mater et al. (2015) and Scotti (2015) explored the veracity of this long-used approach in a variety of conditions. Typically however, this has been examined in the deep ocean and so biased away from the more energetic conditions.

The present paper uses microstructure and overturn data to report on the stratified boundary layer response and mixing in the unique situation of Cook Strait as an aid extending our knowledge around oceanic turbulence. A number of questions arise: (i) Do we see actually observe high dissipation rates? (ii) How does the Thorpe Scale compare with the Ozmidov Scale? (iii) Following from this, can a fixed ratio be assumed and so allow estimation of ε? (iv) How does the turbulence compare with other straits?

2 Location and Sampling

Cook Strait, the channel separating New Zealand's North and South Islands, connects the eastern Tasman Sea to the Western Pacific at 42 S. At its narrowest point it is 22 km across, with 210 and 350 m average and maximum depths, respectively. Its fast-flowing tidal currents have been the focus of a number of studies, including the notable observation that the semidiurnal tide is around 140 degrees out of phase when considering the opposite ends of the Strait (Heath, 1978). This phase difference drives substantial flows, reaching as high as 3.4 m s^{-1} during spring tides (Stevens et al. 2012).

Background velocity data come from two instrumented moorings deployed at the "third points" across the narrows for a period spanning two years, in two deployments, starting in August 2010 and continuing through until September 2012. Each mooring contained an upwards-looking Teledyne-RDI 75 kHz ADCP mounted in a Flotation Technologies syntactic foam float and moored with 600 kg of iron and 10 m of chain. The ADCPs logged at 10 minute intervals, sampling into 8 m depth bins. Each float contained a Seabird microcat (SBE 39)

Ocean Sci. Discuss., doi:10.5194/os-2017-30, 2017
Manuscript under review for journal Ocean Sci.
Discussion started: 15 May 2017

conductivity/temperature/depth sensor placed beneath the ADCPs. The microcats were sampled at 5 minute intervals. This enabled comparison with satellite-derived sea surface temperature for the centre of the strait. With such high flow rates it is not possible to adequately moor instrumentation near the surface as the mooring is "knocked down" meaning that near-surface data are not observed during high flows.

Microstructure profiles were recorded with a VMP500 (Vertical Microstructure Profiler - Rockland Oceanographic, Victoria Canada) instrument. This free-fall loose-tether package supported two shear probes, two fast thermistors, accelerometers and a Seabird Electronics (SBE) conductivity and temperature sensor-pair. Thirty-four profiles were collected using the 14 m twin-hulled jet-boat Ikatere during a number of expeditions from 2008-2012. It is a particularly challenging environment to profile in, due to the fast flows and strong winds, combined with the relatively long profile durations. A profile and retrieval pair would take around 30 minutes to complete, in which time the vessel would have shifted several km. Keeping the vessel on station was not possible as the line would pay out too far and free-fall would cease. Consequently, sequences of two to three profiles were recorded before repositioning was required.

Other sampling strategies have been considered, both as a comparison and as a way to extend the dataset. Ocean glider-mounted microstructure would be affected by the substantial vertical flows. Bed-mounted turbulence sampling will be subject to mooring blow-down so that the sampling package will be constantly moving through the vertical. Surface-floating gear is affected by the very substantial surface wave field and free-drifting mooring-based sampling is unlikely to get regulatory approval due to the potential for fouling on submarine high voltage DC cables that cross the strait.

Traditional microstructure profiling thus appears to be a relatively suitable option for now as we seek to capture a greater variety of conditions, especially during the spring tides. The fast flows mean an ability to rapidly reposition is thus an advantage, meaning a smaller vessel in good weather was a better option than a larger vessel able to handle rougher conditions. The end result of all the trade-offs was that we have yet to work out a way to

Ocean Sci. Discuss., doi:10.5194/os-2017-30, 2017
Manuscript under review for journal Ocean Sci.
Discussion started: 15 May 2017

capture a regular sequence of profiles through a tidal cycle in effectively the same location. However we have built up a dataset through all phases of the tide, though only from a limited set of seasonal conditions and not in the very fastest flows.

The profiler captures temperature and conductivity data, however this sensor-pair is un-pumped (to reduce vibration contamination of the shear probe) and so has a slow actual response and is relatively sensitive to spiking. A fast response conductivity sensor was included in the measurements which gets around the response issue but had its own idiosyncrasies and will not be examined here. Correcting un-pumped salinity estimates is becoming more common with ocean glider applications (Timmermans and Winsor, 2013), however the present profiling application is a more rigorous challenge. Being a derivative quantity, N^2 emphasises any spikes or noise. The bulk temperate-salinity relationship for the region is relatively well-ordered and so this enables density for each profile to be calculated using the high quality temperature and this bulk relationship (for that profile). While this would not be particularly reliable for absolute density estimation it is sufficient to generate an estimate of the buoyancy frequency squared N^2. The density profile contains fine-scale overturns and this also results is a challenge for N^2 estimation. Mather et al (2016) review methods for calculating N^2, and here the patch-average N^2 is used based on a density-sorted profile. The removal of salinity spikes from the original profile data was found to have the greatest impact on the N^2 estimation.

The microstructure data were processed in the usual ways resolving the dissipation rate ε. The data were separated into dissipation rate estimates from each of a sensor pair using 5m depth bins. An approach that identifies the noise limit in the shear spectrum and then replaces this with a model spectrum is applied although with the generally high dissipation rates this was not a particularly dominant correction.

Having resolved ε and N^2 this then enables a number of derived quantities to be calculated. The Ozmidov scale $L_{Oz}=(\varepsilon/N^3)^{1/2}$ identifies the upper bound at which eddies should “feel” the stratification. One might expect overturns, as identified using the L_T, to be equal to, or smaller than L_{Oz}. Dillon 1982 found xxx. This calculation

Ocean Sci. Discuss., doi:10.5194/os-2017-30, 2017
Manuscript under review for journal Ocean Sci.
Discussion started: 15 May 2017

struggles with low stratification where locally-small N^2 drives a very large scale. This makes sense as weak stratification fails to retard turbulence but it can be non-physical as the scale will eventually exceed water depth. The vertical (~diapycnal) diffusivity K_z is commonly calculated as $K_z=\Gamma\varepsilon/N^2$ with $\Gamma=0.2$ an assumed constant. While convenient, there is a good deal of evidence to suggest that Γ is not constant and varies between X & Y. This will be returned to in the Discussion.

Given the nature of the salinity structure, as with Wesson and Gregg (1994) and others, we use the more precisely-known temperature to define overturns. The Thorpe scale L_T is often taken to be some average of displacement scales over a given depth bin. However, this fails to recognise that the enclosed nature of an overturn can set a natural envelope to the estimation (Mather et al 2015) so that moving through the profile and summing displacements, one can see the start of an overturn and then maintain the sum displacements until the nett displacement is brought back to zero within some error. This has the same effect as the centred length scale proposed by Imberger and Boahash (1986) whereby displacements were aggregated at the centre of the overturn. Also by using the microstructure temperature sensor record, the lower limit to this scale is not as limited by spatial resolution, as it is with a traditional CTD thermistor sensor.

3 Results

The nature of the high flow rates in the strait is illustrated with a day-long sub-section of the two years of velocity data from the eastern side of the Strait (Figure 3). The relatively poor data depth coverage is due to instrument tilt, which while remaining within usable tolerances, does exacerbate side-lobe interference from the surface. While predominantly north-south, the vector sum indicates local speeds reaching 3 m s^{-1} at a water depth of around 30 m (speeds above are not known). The flow at this location is not symmetric, with southward flows being 20-50 % smaller.

Ocean Sci. Discuss., doi:10.5194/os-2017-30, 2017
Manuscript under review for journal Ocean Sci.
Discussion started: 15 May 2017

Vertical velocities reach 0.1 m s^{-1} with greater high frequency variability when compared to the horizontal flow signal. Backscatter structure has some correlation to the flow speed, with the fast flow periods heralding increased backscatter through most of the measured water column. The bulk velocity shear is described in Stevens (2014) and the asymmetry is particularly clear with levels reaching maximum values of +/- 0.01 s^{-1}.

The comparison with moored data (Figure 4) suggests that, despite the energetic nature of the strait, it is not fully mixed during the austral summer (Stevens, 2012). The data are insufficient to indicate if the strait is often stratified in density but it is clearly not homogeneous in temperature for a significant portion of the year. Temperature differences between bed and surface are as large as 3 ^{o}C (primarily in the November-April period). Considering the same data in T-S space (Figure 5) shows the seabed and surface temperatures span the same range essentially. Three selected microstructure profiles (A, B and C) demonstrate the vertical structure with vertical density differences reaching as high as 0.5 kg m^{-3} over the full depth of the water column. The low salinity data (S<~ 34.4) is seen in Stevens (2014) and appears to be a 5 month long period at the start of 2012 where the eastern mooring sustained lower S but kept a similar T to other moorings at the time. The profiles come from right at the end of this period and so do not exhibit salinities out of the ordinary.

Before considering the turbulence data en-masse, it is useful to look at the details of some individual profiles. The example profile A (Figure 5) is one of the more strongly stratified observed in the strait. The details of this profile (Figure 7) illustrate the effect of the conductivity sensor being un-pumped. However, the profile structure at the macroscale is monotonic in temperature and so temperature displacements are dynamically meaningful. Stratification persisted throughout the water column with N^2 being around 10^{-5} s^{-2}. Consistent with the relatively constant N^2, the dissipation rate structure through the water column didn't vary greatly. Near-surface values of ε were low, but increased to hold a near-constant level through most of the water column, then rising near the bed. The large central overturn, as identified with the Thorpe analysis, contained the majority of the vertical variability in ε in the profile supporting the decision to keep L_T and ε calculations separate. Diffusivity

Ocean Sci. Discuss., doi:10.5194/os-2017-30, 2017
Manuscript under review for journal Ocean Sci.
Discussion started: 15 May 2017

will be focused on in the Discussion, however it is notable that in this one instance, the combined ε and N^2 imply K_z exceeds 0.1 m^2s^{-1}, i.e. large.

The profile B (Figure 8) differs from profile A in that it has a large quasi-homogeneous upper portion of the water column. Stratification results in a reduced N^2 being as low as 10^{-7} s^{-2} but increasing with depth. The dissipation rate structure increased with depth through the water column (i.e. in tandem with the stratification). The weak stratification was still sufficient that overturn scales were small throughout the water column except for the large upper overturn that exceeds 80 m in scale. Interestingly this coincided with an upper layer of *low* dissipation rate. However, this may be due to a thin low salinity surface layer with a compensating low temperature, and is a case where density rather than temperature should be used. In this example, the combined ε and N^2 imply a K_z peaking at around 0.1 m^2s^{-1} but mostly an order of magnitude smaller.

The final profile example described here, profile C (Figure 9), sustains a lower quasi-homogeneous region of the water column. Stratification results in N^2 having a baseline around 10^{-6} s^{-2} but significantly increasing at the interface zones. The dissipation rate structure here is bi-modal with a mid-depth minimum. Overturn scales followed the dissipation rate trend with an especially large structure near the bed. Dissipation rates at the bed exceeded $5x10^{-6}$ W kg^{-1}. The variability in ε dominates that of the N^2, so that the K_z structure mirrors ε closely with K_z peaking just under 1 m^2s^{-1} near the bed.

4 Discussion

Are the dissipation rates actually large?

The distribution of dissipation rate (Figure **10**a) shows the level of turbulent kinetic energy (as inferred by ε) extends over five orders of magnitude. While the linear average is around $2x10^{-6}$ W kg^{-1} extrema can exceed 10^{-4} W kg^{-1}. In addition, most unusually, there were almost no estimates down at the instrument noise floor around

Ocean Sci. Discuss., doi:10.5194/os-2017-30, 2017
Manuscript under review for journal Ocean Sci.
Discussion started: 15 May 2017

10^{-10} W kg^{-1}. Scaling these estimates over depth, taking the perspective of a numerical modeller looking to resolve friction losses through a Strait, suggests between 0.6 and 30 W m^{-2} are lost through turbulent dissipation (c.f. say Bab el Mandab of a maximum around 0.2 W m^{-2}, Jarosz et al. 2005).

It is easy to ignore bulk Re in ocean physics, assuming correctly that any Re calculation will be "large". However, at the turbulence scales buoyancy can potentially affect overturns and re-stratification. The turbulent buoyancy Reynolds number Re_b ($=\varepsilon/[\nu N^2]$) identifies how velocity fluctuations, and any associated buoyancy flux, evolves and decay. In the present Cook Strait data, the majority of Re_b estimates exceed two orders of magnitude with the peak of the distribution around $5x10^4$. (Figure **11**). However, maximal values exceed 10^7, which is primarily due to the small *N*. This is larger than the range observed by Wesson and Gregg (1994) who saw more values around 10^2-10^3, but still with high values reaching 10^5 or more.

Does the Thorpe Scale vary systematically with the Ozmidov Scale?

A cross-comparison of L_T with L_{Oz} (Figure **12**) shows a systematic co-variation but one that is far from 1:1. No L_T greater than 100 m were observed despite the water column exceeding three-times this and with weak stratification. L_{Oz} on the other hand is not actually physically constrained and in several instances it exceeds the water depth. Considering $\log_{10}$ distributions of L_T with L_{Oz}, the observed Thorpe displacement scale L_T is substantially smaller than the buoyancy-controlled limit L_{Oz}, by an order of magnitude at smaller length-scales. The two estimates come closest at around L_T~ 10m (being around 50% of L_{Oz}).

Wesson and Gregg's (1994) observations of turbulence quantities in the Strait of Gibraltar find that the L_{Oz} (L_B in their notation) compares essentially 1:1 with L_T, with most estimates falling within a factor of 4 either side. They also found this degree of scatter held throughout the water column. This differs from that seen here (Figure 12) where the L_T is substantially smaller than the L_{Oz} by as much as a decade at smaller scales. The scatter is also larger in the present data as this also is around a decade either side of the mean value. This latter point

Ocean Sci. Discuss., doi:10.5194/os-2017-30, 2017
Manuscript under review for journal Ocean Sci.
Discussion started: 15 May 2017

may be driven by the method used to calculate L_T. The present noise-rejection conditions mean that there are fewer very small L_{Oz} (say <0.5 m) whereas the Gibraltar data drop to as low as 10^{-2} m. The present Cook data exhibit a possible split in behaviour around L_{Oz}=10 m whereas the Gibraltar data only hints at this. Making the same comparison with the Dunkley et al. (2015) Gulf of Aqaba observations ranging over L_T=0.1-10 m, the distribution is almost a mirror reflection around the 1:1 line from that observed in Cook Strait. In the Gulf of Aqaba results, the L_T exceeds on average the L_{Oz} by as much as an order of magnitude. Bluteau et al (2013) data show a similar trend.

One of the challenges in ocean turbulence is that studies are so intense, focused and idiosyncratic that they tend to be analysed in isolation and rarely synthesized. Mater et al. (2015) collated three open-ocean turbulence experiments from (i) the North Atlantic at around 3000 m (NATRE, Toole et al. 1994), (ii) Brazil Basin mid-Atlantic at around 3000 m (BBTRE, St. Laurent et al. 2001) and (iii) Luzon Straits at around 2500-3000m, (IWISE, Alford et al 2011). Here we consider the present data in this context (Figure 13). The ratio of L_T to L_{Oz} in these deep water experiments was considered against a L_T non-dimensionalised by the length scale extracted from viscosity and buoyancy $(\nu/N)^{1/2}$. All follow the same trend of the ratio L_T/L_{Oz} growing with increasing eddy size. All but the NATRE data have significant proportion of data lying with $L_T < L_{Oz}$. The present Cook Strait data illustrate this aspect most strongly nearing an order of magnitude smaller at low L_T. Furthermore, the present data extend into the largest non-dimensional L_T space. Mater et al. (2015) suggest that while the experiments are deep-water they are still constrained vertically by convective scales.

Does L_{Oz}/L_T allow estimation of ε?

A comparison of dissipation rate estimated ε and the Thorpe Scale L_T indicates comparable trend but that the comparison is not 1:1 (Figure 12) with the departure growing for larger scales. There looks to be a bias towards high L_T values for low L_{Oz} value at shallow depths. Using the Dillon (1982) approach of assuming taking the $L_{Oz}=[\varepsilon/N^3]^{1/2}$ and assuming L_{Oz}/L_T is fixed such that $L_{Oz}=aL_T$ then we arrive at a simple expression for

Ocean Sci. Discuss., doi:10.5194/os-2017-30, 2017
Manuscript under review for journal Ocean Sci.
Discussion started: 15 May 2017

ε (Figure 14). This compares the dissipation rates from each L_T overturn with both the direct and log10-based average ε within that overturn. The direct average (squares) provides a close comparison between observed and estimated ε. This agreement holds from $2x10^{-9}$ W kg^{-1} through to $2x10^{-5}$ W kg^{-1}, with only one or two departures. The most notable being at 10^{-9} W kg^{-1} where it is biased high by a very larger outlier that should possibly be discounted. There is an obvious family of outliers in the upper 30 m of water that are anomalously high in terms of the parametrised estimate $a^2L_T^2N^3$ of dissipation rate. Most likely this is a result of some surface-driven stratification effect that either (i) affects turbulence in some systematic way, or (ii) confounds the temperature-based density correction. The log-based comparison is around an order of magnitude smaller. This is included in order to compare this representation with Figure **12**.

Implications for, and of, diapycnal diffusion estimates

Extending this by applying the Osborne diffusivity method sees an average diffusivity is around 0.04 m^2 s^{-1} and exceeding 1 m^2 s^{-1} (Figure **10**b). One might expect a 300 m water column to then be homogenised in a time (L^2/K_z=) $300^2/1$=25 hours. Tidal excursions due to the semidiurnal tide are insufficient to flush the strait in a single cycle. Indeed, with a net drift of around 0.02-0.1 m s^{-1} (Stevens 2014) it takes many tidal cycles. This suggests that, at these most energetic of mixing conditions, we should not expect to see a stratified water column as it should get mixed over the multiple tidal cycles it takes for water to clear the strait. The bulk top-bottom observations (Figure 4) counter this as, for some of the year at least, there is clearly a scalar gradient. The Γ=0.2 "constant" is a clear point of contention in the literature (e.g. Bluteau et al. 2013; Mashayek et al. 2013) however given the present high Re it is likely less of an issue.

Lafuente et al. (2013), in their exploration of vertical diffusion of biologically relevant scalars in the Straits of Gibraltar, found a highly two-dimensional situation whereby the mixing is highly spatially variable with the presence and location of an internal hydraulic jump being very important. In a similar way to Cook Strait,

Ocean Sci. Discuss., doi:10.5194/os-2017-30, 2017
Manuscript under review for journal Ocean Sci.
Discussion started: 15 May 2017

their simulations show, despite the reasonable tides and strong estuarine circulation, it takes some time for well-mixed water to exit the system. Lafuente et al. (2013) set their background vertical diffusivity to 10^{-7} m^2 s^{-1} and also prescribed a maximum of 10^{-2} m^2 s^{-1} in order to "avoid unrealistically high values". While having the potentially very small N^2 in the denominator for K_z is problematic, the very large ε and L_T make it reasonable to assume, with finite N, that the larger K_z are robust.

How does the turbulence compare with other straits?

It is instructive to compare Cook Strait with other straits of note (Table 1). When doing so it is worth being mindful that Gregg & Özsoy (2002) quoted Tolstoy when relating the unique nature of any given strait. The Tolstoy quote was in the context of the Bosphorus, the canonical strait at this scale is probably Gibraltar, the scene of some of the first systematic turbulence quantification (Wesson and Gregg, 1994). Cook Strait, being essentially oceanic, is relatively weakly stratified, with the g' in Table 1 being a maximum as observed through an annual cycle.

Wesson and Gregg (1994) state that "rather than being definitive, these results are only the beginning of turbulence measurements in the Strait of Gibraltar". While this has not really turned out to be the case for Gibraltar, the approach and results spawned a range of studies in comparable systems, with the ensemble providing a natural laboratory for exploring aspects of ocean mixing. In Cook Strait, with its remarkable tides, we intend to improve operational techniques to see if it is possible to sample during the fastest of the spring tides in order to capture turbulence data in even higher bulk Reynolds number conditions.

Acknowledgements

The author would like to acknowledge colleagues who have aided in the work, in particular Brett Grant, Mark Hadfield, Fiona Elliott, Craig Stewart, Ross Vennell, Murray Smith, Steve Chiswell, Graham Rickard, Rebecca McPherson and Joanne O'Callaghan. The support of NIWA Core Funding and the New Zealand Sustainable Seas National Science Challenge is acknowledged.

5 References

Bluteau, C. E., N. L. Jones, and G. N. Ivey (2013), Turbulent mixing efficiency at an energetic ocean site, J. Geophys. Res. Oceans, 118, 4662–4672, doi:10.1002/jgrc.20292.

Bowman, M.J., A.C. Kibblewhite, S.M. Chiswell and R. Murtagh, 1983b: Shelf fronts and tidal stirring in Greater Cook Strait, New Zealand. Oceanologica Acta 6, 119-129.

Bryden, H.L. and Nurser, A.G., 2003. Effects of strait mixing on ocean stratification. *Journal of Physical Oceanography*, *33*(8), pp.1870-1872.

Dale, A. C., and M. E. Inall (2015), Tidal mixing processes amid small-scale, deep-ocean topography, Geophys. Res. Lett., 42, 484–491, doi:10.1002/2014GL062755.

Dillon, T.M., 1982. Vertical overturns: A comparison of Thorpe and Ozmidov length scales. *Journal of Geophysical Research: Oceans*, *87*(C12), pp.9601-9613.

Dunckley, J. F., J. R. Koseff, J. V. Steinbuck, S. G. Monismith, and A. Genin (2012), Comparison of mixing efficiency and vertical diffusivity models from temperature microstructure, J. Geophys. Res., 117, C10008, Doi:10.1029/2012JC007967.

Finnigan, T. D., D. S. Luther, and R. Lukas, 2002. Observations of enhanced diapycnal mixing near the Hawaiian Ridge. J. Phys. Oceanogr., 32;2988–3002.

Frants, M., Damerell, G. M., Gille, S. T., Heywood, K. J., MacKinnon, J., & Sprintall, J. (2013). An assessment of density-based finescale methods for estimating diapycnal diffusivity in the Southern Ocean. *Journal of Atmospheric and Oceanic Technology*, *30*(11), 2647-2661.

Garrett, C., 2004. Frictional processes in straits. *Deep Sea Research Part II: Topical Studies in Oceanography*, *51*(4), pp.393-410.

Heath R.A., 1978: Semidiurnal tides in Cook Strait. New Zealand Journal of Marine and Freshwater Research, 12, 87–97.

Helfrich, K.R., 1995. Time-dependent two-layer hydraulic exchange flows. *Journal of Physical Oceanography*, *25*(3), pp.359-373.

Hogg, A.M., Ivey, G.N. and Winters, K.B., 2001. Hydraulics and mixing in controlled exchange flows. *Journal of Geophysical Research: Oceans*, *106*(C1), pp.959-972.

Imberger, J., & Boashash, B. (1986). Application of the Wigner-Ville distribution to temperature gradient microstructure: A new technique to study small-scale variations. *Journal of physical oceanography*, *16*(12), 1997-2012.

Lafuente, J. G., Pozas, E. B., Garrido, J. C. S., Sannino, G., & Sammartino, S. (2013). The interface mixing layer and the tidal dynamics at the eastern part of the Strait of Gibraltar. *Journal of Marine Systems*, *117*, 31-42.

Mashayek, A., Caulfield, C.P. and Peltier, W.R., 2013. Time-dependent, non-monotonic mixing in stratified turbulent shear flows: Implications for oceanographic estimates of buoyancy flux. Journal of Fluid Mechanics, 736, pp.570-593.

Mater, B.D., Schaad, S.M. and Venayagamoorthy, S.K., 2013. Relevance of the Thorpe length scale in stably stratified turbulence. *Physics of Fluids (1994-present)*, *25*(7), p.076604.

Mater, B. D., & Venayagamoorthy, S. K. (2014). A unifying framework for parameterizing stably stratified shear-flow turbulence. *Physics of Fluids (1994-present)*, *26*(3), 036601.

Scotti, A., 2015. Biases in Thorpe-scale estimates of turbulence dissipation. Part II: energetics arguments and turbulence simulations. *Journal of Physical Oceanography*, *45*(10), pp.2522-2543.

Stevens, C.L., M.J. Smith, B. Grant, C.L. Stewart, and T. Divett, 2012: Tidal stream energy extraction in a large deep strait: the Karori Rip, Cook Strait, Continental Shelf Research, 33, 100-109.

Stevens, C., 2014. Residual flows in Cook Strait, a large tidally dominated strait. *Journal of Physical Oceanography*, *44*(6), pp.1654-1670.

Stewart, R.W. and Grant, H.L., 1999. Early measurements of turbulence in the ocean: Motives and techniques. *Journal of Atmospheric and Oceanic Technology*, *16*:1467-1473.

St. Laurent, L. C., Toole, J. M., & Schmitt, R. W. (2001). Buoyancy Forcing by Turbulence above Rough Topography in the Abyssal Brazil Basin*. Journal of Physical Oceanography, 31(12), 3476-3495.

Thorpe, S. A. 1977. Turbulence and mixing in a Scottish loch, Philosophical Transactions of the Royal Society of London, A286: 125-181.

Timmermans, M. L., & Winsor, P. (2013). Scales of horizontal density structure in the Chukchi Sea surface layer. *Continental Shelf Research*, *52*, 39-45.

Vennell, R. 1994: Acoustic Doppler Current Profiler measurements of tidal phase and amplitude in Cook Strait, New Zealand, Continental Shelf Research, 14, 353-364.

Vennell, R., 1998. Observations of the phase of tidal currents along a strait. *Journal of physical oceanography*, *28*(8), pp.1570-1577.

Waterhouse, A.F., MacKinnon, J.A., Nash, J.D., Alford, M.H., Kunze, E., Simmons, H.L., Polzin, K.L., St. Laurent, L.C., Sun, O.M., Pinkel, R. and Talley, L.D., 2014: Global patterns of diapycnal mixing from measurements of the turbulent dissipation rate. Journal of Physical Oceanography, 44, 1854-1872.

Ocean Sci. Discuss., doi:10.5194/os-2017-30, 2017
Manuscript under review for journal Ocean Sci.
Discussion started: 15 May 2017

Wesson, J. C., and M.C. Gregg, 1994: Mixing at Camarinal Sill in the Strait of Gibraltar, J. Geophys. Res., 99, 9847–9878.

Ocean Sci. Discuss., doi:10.5194/os-2017-30, 2017
Manuscript under review for journal Ocean Sci.
Discussion started: 15 May 2017

Table 1 Comparison of strait scales (modified from Helfrich, 1995)

Strait	g' $m\ s^{-2}$	Depth m	U $m\ s^{-1}$	Length km	Re	G^2	Ri
Cook	0.006	350	3.0	40	10^9	~2.5	0.9
Bosphorus	0.12	35	0.8	30	$3x10^7$	-	2.1
Georgia (Cordova)		(avg) 156	~	220		-	
		30	0.9	3	$3x10^7$	-	
Gibraltar	0.02	280	1.2 (M_2)	20	$4x10^8$	-	3.6

Ocean Sci. Discuss., doi:10.5194/os-2017-30, 2017
Manuscript under review for journal Ocean Sci.
Discussion started: 15 May 2017

Ocean Science
Discussions
Open Access
EGU

Figures

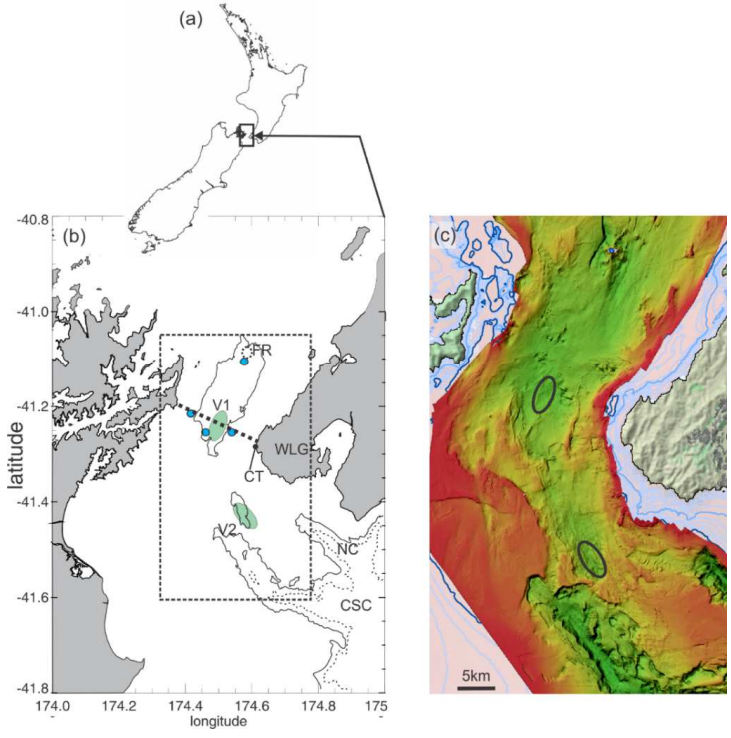

Figure 1 Location showing (a) New Zealand, and within this, (b) Cook Strait Narrows is bounded by Cape Terawhiti (CT) to the east and the headlands of the (shaded) Marlborough Sounds to the west and with the Cook Strait and Nicholson Canyons to the south (CSC and NC). The 200 m (solid) and 400 m (dashed) depth contours are marked, as well as the shoal at Fishermans Rock (FR). ADCP moorings are marked with blue circles. The microstructure data come from profile regions V1 and V2.

Ocean Sci. Discuss., doi:10.5194/os-2017-30, 2017
Manuscript under review for journal Ocean Sci.
Discussion started: 15 May 2017

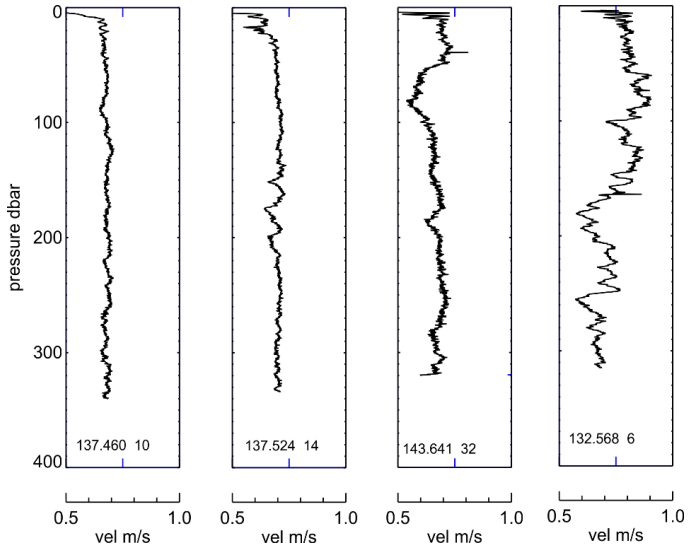

Figure 2 profiler drop speed from a number of example profiles.

Ocean Sci. Discuss., doi:10.5194/os-2017-30, 2017
Manuscript under review for journal Ocean Sci.
Discussion started: 15 May 2017

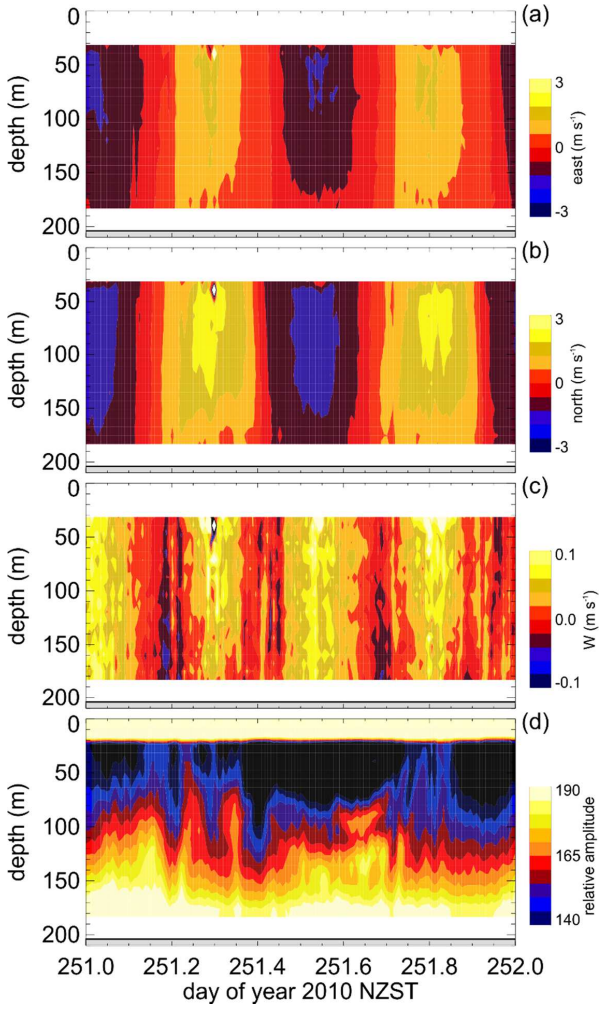

Figure 3 velocity data from eastern side of strait showing (a) east-west, (b) north -south, (c) vertical velocities and (d) backscatter amplitude.

Ocean Sci. Discuss., doi:10.5194/os-2017-30, 2017
Manuscript under review for journal Ocean Sci.
Discussion started: 15 May 2017

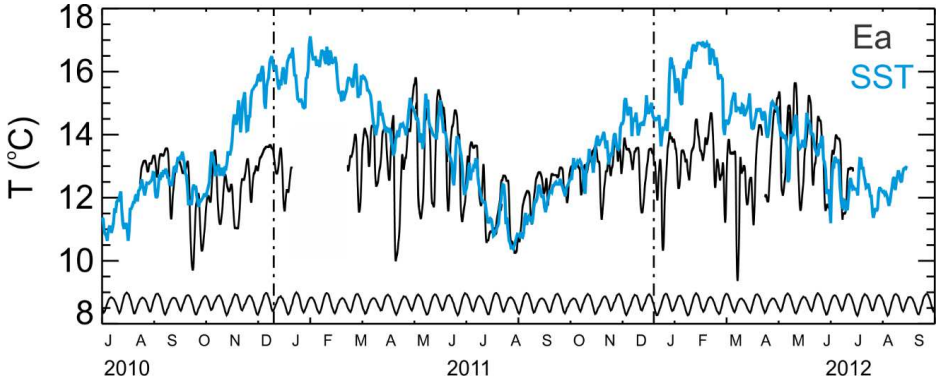

Figure 4 Temperatures from near-bed (Ea, Figure 1) and satellite-derived sea surface temperature (SST). The arbitrarily-scaled spring-neap envelope is along the base of the panel.

Ocean Sci. Discuss., doi:10.5194/os-2017-30, 2017
Manuscript under review for journal Ocean Sci.
Discussion started: 15 May 2017

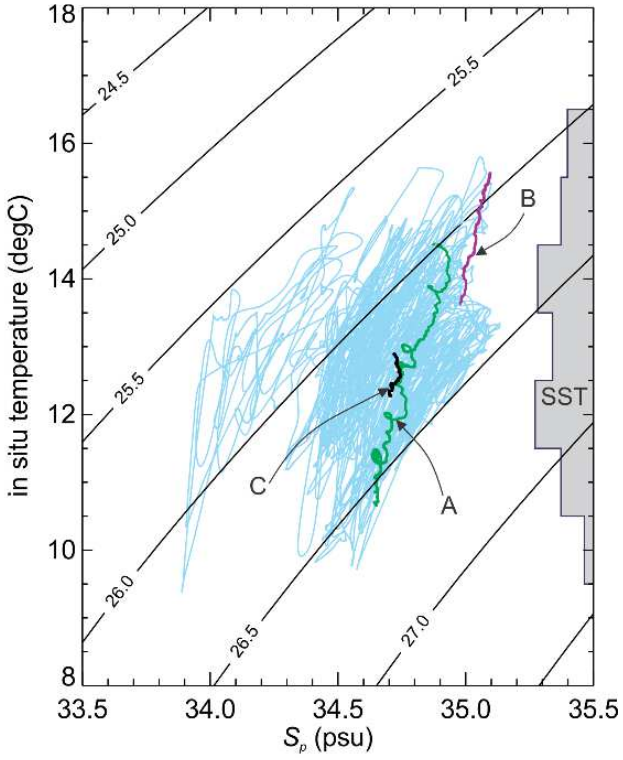

Figure 5 Temperature and salinity (S_p) from the seabed sensors on the moorings with profile data overlain (see text for details) and σ_T contours. The arbitrary-scaled distribution on the right-hand margin shows the distribution of satellite-derived sea surface temperature (SST).

Ocean Sci. Discuss., doi:10.5194/os-2017-30, 2017
Manuscript under review for journal Ocean Sci.
Discussion started: 15 May 2017

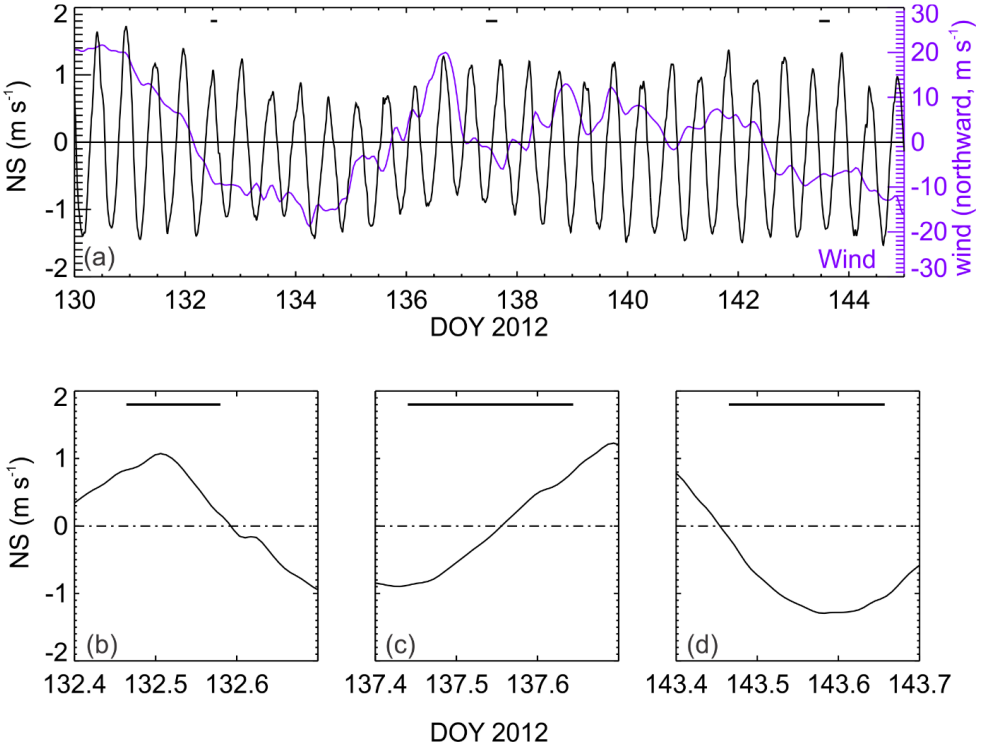

Figure 6 sampling conditions average N-S velocity between 60 and 100 m depth and wind speed both filtered with an hourly low-pass filter. The bars show sample periods.

Ocean Sci. Discuss., doi:10.5194/os-2017-30, 2017
Manuscript under review for journal Ocean Sci.
Discussion started: 15 May 2017

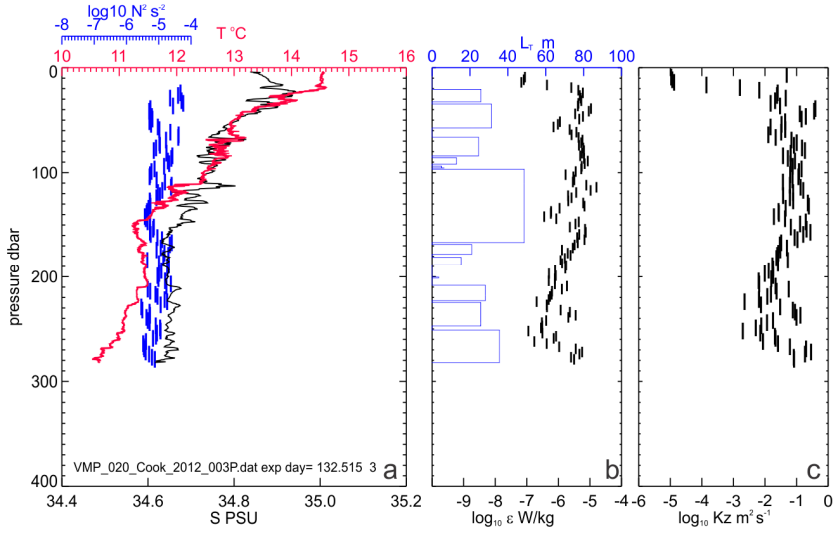

Figure 7 Profile A from day 132, 2012 showing (a) temperature, salinity and buoyancy frequency (N^2) squared, (b) L_T and ε and (c) vertical diffusivity K_z. Note the profile extends over the full depth of the water column.

Ocean Sci. Discuss., doi:10.5194/os-2017-30, 2017
Manuscript under review for journal Ocean Sci.
Discussion started: 15 May 2017

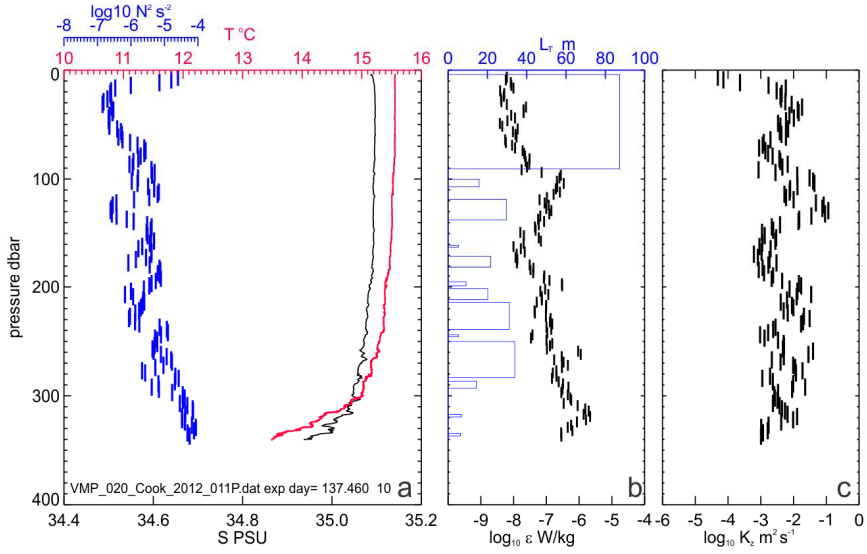

Figure 8 Profile B from day 137, 2012 showing (a) temperature, salinity and buoyancy frequency (N^2) squared, (b) L_T and ε and (c) vertical diffusivity K_z. Note the profile extends over the full depth of the water column.

Ocean Sci. Discuss., doi:10.5194/os-2017-30, 2017
Manuscript under review for journal Ocean Sci.
Discussion started: 15 May 2017

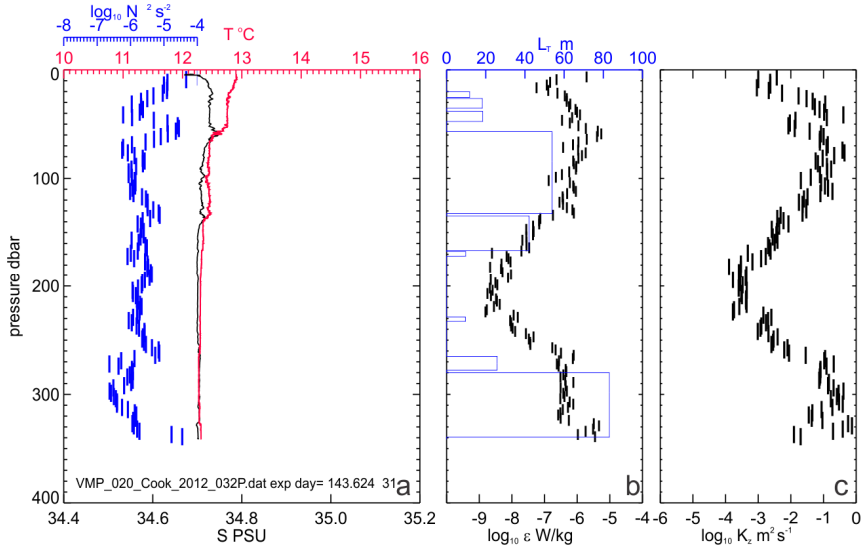

Figure 9 Profile C from day 143, 2012 showing (a) temperature, salinity and buoyancy frequency (N^2) squared, (b) L_T and ε and (c) vertical diffusivity K_z. Note the profile extends over the full depth of the water column.

Ocean Sci. Discuss., doi:10.5194/os-2017-30, 2017
Manuscript under review for journal Ocean Sci.
Discussion started: 15 May 2017

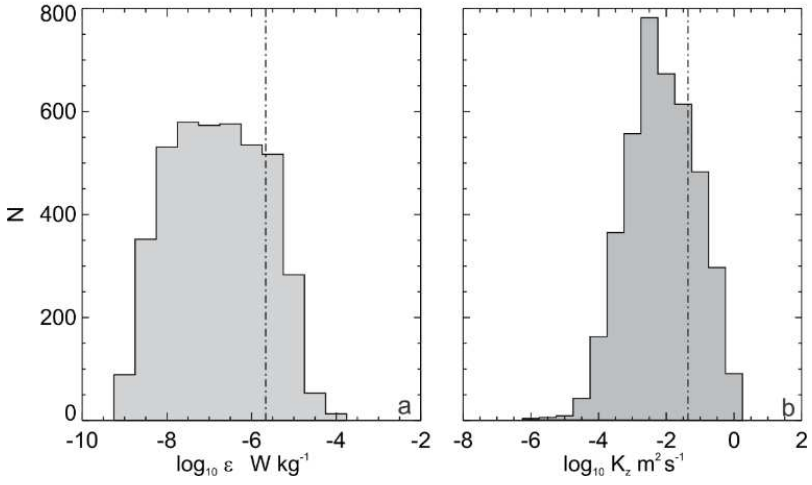

Figure 10 Distributions of (a) dissipation rate ε and (b) inferred vertical diffusivity K_z.

Ocean Sci. Discuss., doi:10.5194/os-2017-30, 2017
Manuscript under review for journal Ocean Sci.
Discussion started: 15 May 2017

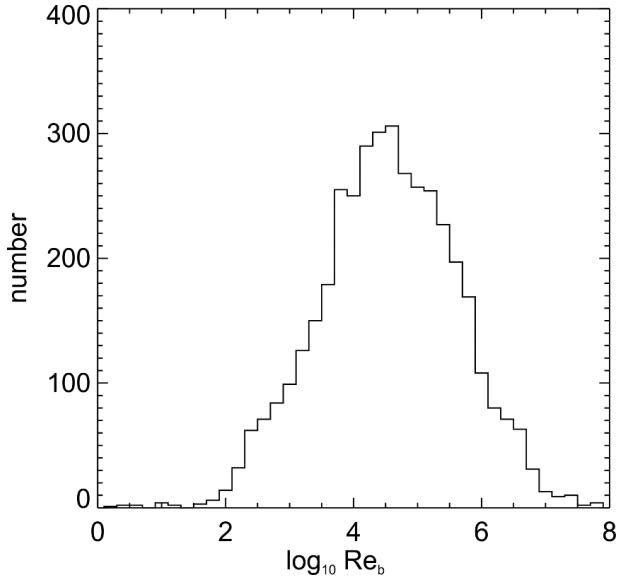

Figure 11 Distribution of buoyancy Reynolds number, Re_b.

Ocean Sci. Discuss., doi:10.5194/os-2017-30, 2017
Manuscript under review for journal Ocean Sci.
Discussion started: 15 May 2017

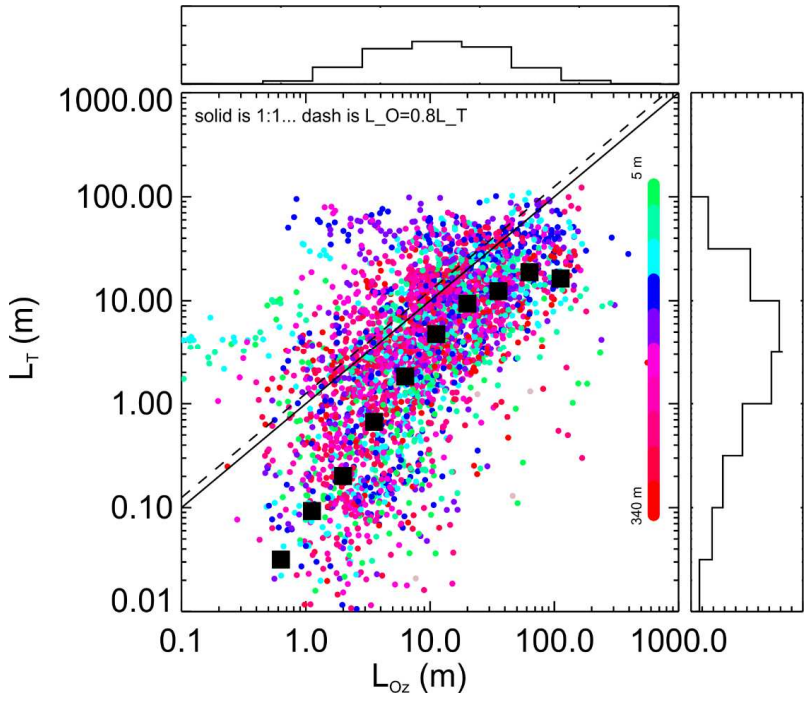

Figure 12 Scatter plot of L_T vs L_{Oz} colour-coded by depth. Lines for unity and for $L_{Oz}=0.8L_T$ are shown and associated histograms of length-scales are shown also. Averages were calculated in log10 space and 0.5 m was considered a lower-bound for L_{Oz}.

Ocean Sci. Discuss., doi:10.5194/os-2017-30, 2017
Manuscript under review for journal Ocean Sci.
Discussion started: 15 May 2017

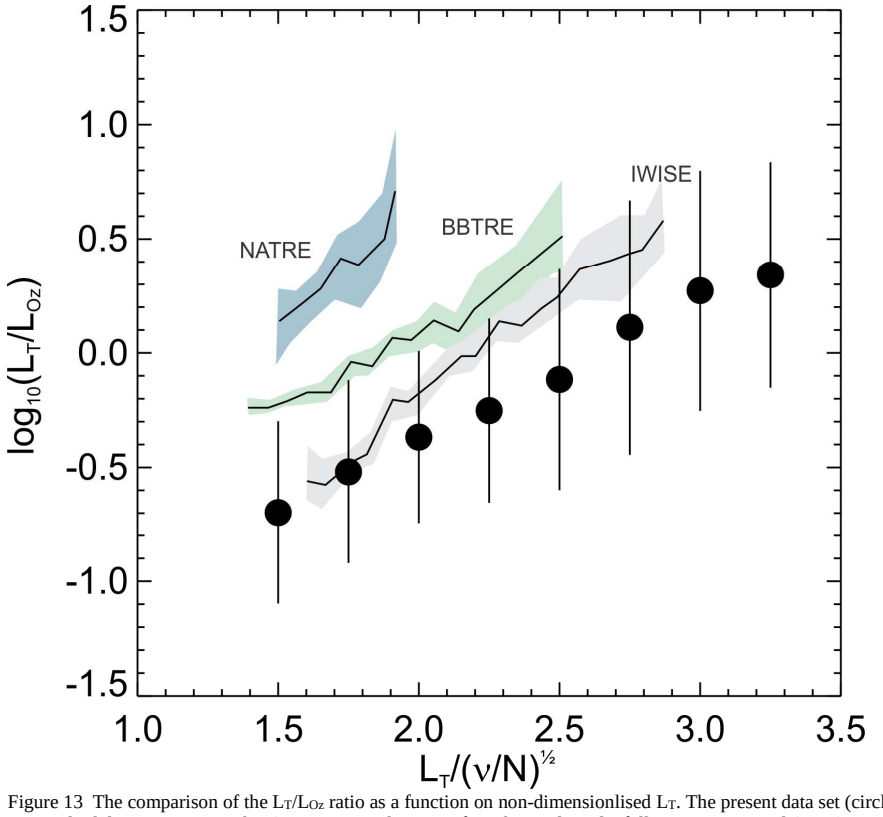

Figure 13 The comparison of the L_T/L_{Oz} ratio as a function on non-dimensionlised L_T. The present data set (circles with +/- 1x standard deviation as error bars) is superposed on top of synthesized results following Mater et al (2015).

Ocean Sci. Discuss., doi:10.5194/os-2017-30, 2017
Manuscript under review for journal Ocean Sci.
Discussion started: 15 May 2017

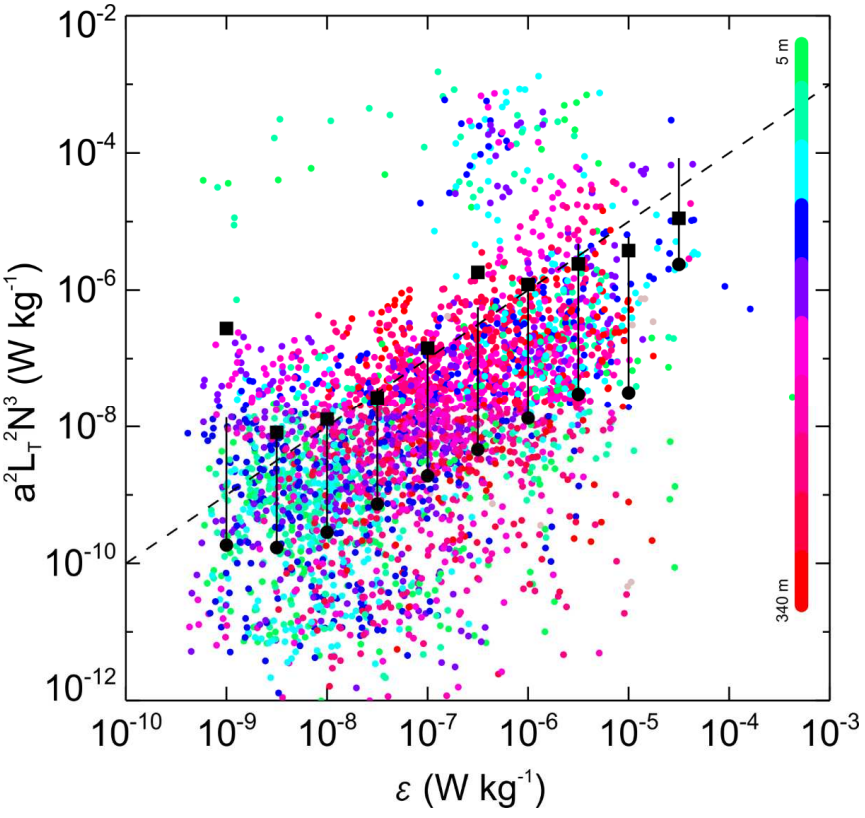

Figure 14 Comparison of dissipation resolved from the L_{Oz} with the direct measure of ε. Averages were calculated in log10 space for ε and all length-scale-based estimates in that bin were collated. Here the average and average+ 1 standard deviation are shown with a circle-line pair and the average in log10 space is shown as a square. The averages excluded outliers in the surface water as described in the text.